NIPES

Journal of Science and Technology Research

Journal homepage: www.nipesjournals.org.ng

Kinetics and Thermodynamics Studies of the Transesterification of Waste Cooking Oil Using Biochar-Based Catalyst Derived from Rubber Seed Shells

Charity Aghariagbonse Osagiede* and Christopher Ehiaguina Akhabue
Department of Chemical Engineering, University of Benin, Benin City, Nigeria
*Corresponding Author Email: aghariagbonse.osagiede@eng.uniben.edu

Article Info

Keywords: *Kinetics, Thermodynamics, Transesterification, Biodiesel, Waste cooking oil*

Received 5 March 2024
Revised 17 May 2024
Accepted 25 May 2024
Available online 30 June 2024

https://doi.org/10.5281/zenodo.12706977

Abstract

Biodiesel, a renewable and environmentally friendly fuel, has gained significant attention as an alternative to conventional diesel due to its numerous advantages, such as reduced greenhouse gas emissions, biodegradability, and sustainability. In this study, the kinetics and thermodynamics of the transesterification of Waste Cooking Oil (WCO) using a recently developed biochar-based catalyst derived from rubber seed shells were investigated. Experimental kinetic data were obtained using UV-spectrophotometric analysis of glycerol concentration. Three kinetic models- power law, Eley-Rideal, and Langmuir-Hinshelwood, were fitted to the experimental data, and their fitness and suitability were assessed using statistical parameters such as coefficient of determination (R^2), adjusted R^2, root mean square error (E_{RMS}), and variance. The results show that the reaction kinetics of the transesterification of WCO over the developed catalyst is best described by the irreversible pseudo-first-order kinetic model, having a rate constant of 0.0164 min^{-1} at 65 °C. The exponential factor and the activation energy of the reaction were 7139.5 min^{-1} and 36.6 kJ/mol respectively. The thermodynamic parameters of the reaction include a change in enthalpy (ΔH) of 33.9 kJ/mol and a change in entropy (ΔS) of -0.180 kJ/mol. K, with positive Gibb's free energy (ΔG) values. The results, therefore, imply that the transesterification of WCO catalyzed by the recently developed biochar-based catalyst derived from rubber seed shells is an endothermic process and a non-spontaneous reaction.

1.0. Introduction

The production of biodiesel from waste cooking oil (WCO) has gained significant attention as a sustainable and cost-effective alternative to conventional diesel fuel [1, 2]. Biodiesel, a renewable and environmentally friendly fuel, offers numerous advantages such as reduced greenhouse gas emissions, biodegradability, and lower dependence on fossil fuels [3, 4].

In recent years, researchers have focused on developing efficient and cost-effective catalysts for the transesterification process in biodiesel production. One promising approach is the utilization of waste materials as catalysts, such as rubber seed shells and eggshells [5, 6]. Rubber seed shell is an abundant agricultural waste product that can be converted into an effective solid base catalyst through thermal activation [7, 8]. Eggshell, on the other hand, is a calcium-rich waste material that can be used as a source of calcium oxide (CaO), a widely used heterogeneous catalyst in biodiesel production [6, 8].

The kinetics and the thermodynamics aspects of transesterification reaction are of great interest to researchers, as they help to understand the energy changes and equilibrium behavior during the reaction process. Several studies [9 – 12] have focused on investigating the thermodynamics of transesterification reactions, with a particular emphasis on activation energy, Gibbs free energy, enthalpy, and entropy changes. The kinetics and thermodynamic behaviour of transesterification of waste cooking oil, using bio-based catalysts is understudied. A recent study reported the use of a biochar-based catalyst derived from rubber seed shells for biodiesel production from waste cooking oil [5]. The emphasis of this study was on catalyst preparation, characterization, biodiesel production, and optimization. No attempt was made to explore the kinetics and thermodynamics of the reaction.

To the best of our knowledge, no detailed study has been previously conducted to explicitly elucidate the kinetics and thermodynamics of the transesterification of waste cooking oil using biochar-based catalyst derived from rubber seed shells. Again, most of the reported kinetics and thermodynamics studies of heterogeneous catalyzed transesterification were conducted using an expensive Gas Chromatography-Mass Spectrometric (GC-MS) analytic approach for data collection [9 – 11, 20]. This study has employed UV-Spectrophotometric analysis of glycerol concentration, an alternative analytical approach that is relatively inexpensive but effective for kinetic data collection. This study, therefore, aims to investigate the kinetics and thermodynamics of the transesterification of waste cooking oil using a recently developed heterogeneous catalyst derived from rubber seed shells and eggshells.

2.0 Materials and Methods

The materials used in the study were locally sourced. Eggshells and WCO were obtained from some local restaurants in Benin City while Rubber seed shells were obtained from the Rubber Research Institute, Iyanomo, Edo State, Nigeria. All the reagents used in this study were of analytic grade.

2.1 Catalyst Preparation

The acid-based bifunctional catalyst (ABFC) was prepared through a sequence of steps that involved carbonization, calcination, and impregnation. Fifty grams of rubber seed shells were carbonized at 600 °C for 4 hours in an inert muffle furnace with a nitrogen supply to produce rubber seed shell biochar. Twenty grams of this biochar were then activated by heating with 200 ml of sulfuric acid for 4 hours, resulting in sulfonated rubber seed shell biochar. Meanwhile, the pretreated eggshells were calcined at 900 °C to produce calcined eggshells. Next, the sulfonated rubber seed shell biochar was impregnated with the calcined eggshells by mixing them in a 3:2 ratio with 150 ml of distilled water and heating to dryness at 105 °C. The dried residue was then recalcined at 700 °C to produce the catalyst.

Detailed catalyst preparation and characterization, as well as WCO characterization procedures, have been reported in our previous study [5].

2.2 Transesterification reaction

The transesterification reaction was performed in a three-neck batch reactor using the optimized reaction conditions of a methanol/oil ratio of 14.2:1 and a catalyst concentration of 2.0 wt.% as reported in our previous study [5]. These conditions were kept constant in all the experimental runs. The experiments were performed in three sets, each conducted at different fixed temperatures (45, 55, and 65 °C). After the start of the reaction, samples were taken every 30 minutes. The collected samples were cooled and then centrifuged to remove catalysts before measuring their glycerol concentration using a UV-Vis Spectrophotometer (Varian, Lake Forest). The concentrations of the other reaction species were derived from glycerol concentrations based on their stoichiometric relationship.

2.3 Preparation of Calibration Curve

The calibration curve was prepared following the method described by Bondioli and Bella [13]. Typically, 0.00, 0.25, 0.50, 0.75, 1.00, 1.25, 1.50, 1.75, and 2.00 mL of a 0.036 g/ml glycerol solution were measured into ten separate test tubes. The content of each test tube was made up to 2 mL by the addition of the working solvent, a solution prepared by mixing an equal volume of water and 95% ethanol. To each of the test tubes, 1.2 ml of a 10 mM sodium periodate solution was added and their contents were thoroughly agitated for a period of 30 min. Thereafter, 1.2 ml of a 0.2 M acetylacetone solution was also added to each of the test tubes, and the test tubes were placed in the water bath at 70 ^{o}C for 1 min to enable the reaction to take place. At the end of the reaction time, the samples were immediately allowed to cool, after which the spectra and absorbance for each of them were measured using a UV-Vis spectrophotometer positioned in a double beam mode at 410 nm.

The resulting calibration curve showing the variation of absorbance with the concentration of glycerol in the samples is presented in Figure 1. This curve was used to determine the concentration of glycerol present in the reaction mixture at any given time. The concentrations of triglyceride, methanol, and FAME were obtained from the concentration of glycerol, based on the stoichiometric relationship between them. The concentrations of the reaction species are stoichiometrically connected by the following expressions: $C_T = C_{TO} - C_G$, $C_F = 3C_G$, and $C_M = C_{MO} - C_G$.

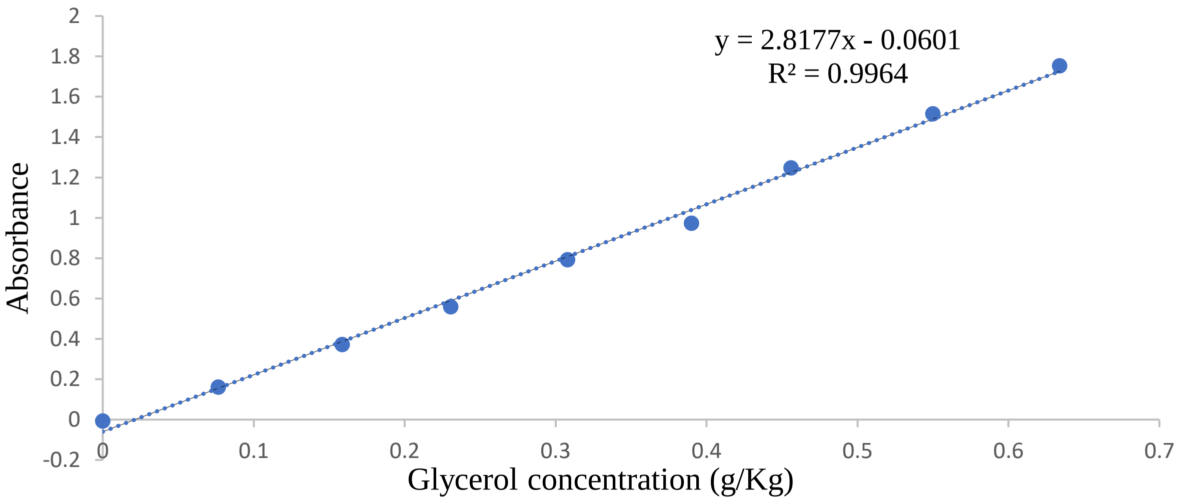

Figure 1: Glycerol concentration calibration curve for 1 kg of sample

2.3 UV-Vis Spectrophotometric Analysis of Glycerol Concentration

The analysis of glycerol in biodiesel is based on the formation of formaldehyde when glycerol reacts with sodium periodate. The subsequent reaction of formaldehyde with acetyl acetone produces yellow complexes, 3, 5-diacetyl-1, 4-dihydrolutidine. The compound is produced proportionately to the quantity of glycerol available for reaction. The measurement of 3, 5-diacetyl-1, 4-dihydrolutidine with a specific adsorption band at 410 nm provides an indirect means of measuring the amount of glycerol in the sample [13, 14].

2.4 Investigation of Reaction Kinetic Models

Different reaction kinetics models were investigated in search of the model that best fit the experimental data. The models tested include power law, Eley-Rideal, and Langmuir-Hinshelwood-Hougen-Watson models. A similar analysis to that used by Al-Sakka [15] in the "Kinetic study of soybean oil methanolysis using cement kiln dust as a heterogeneous catalyst for biodiesel production" was adopted. The derivatives of the accompanied rate equations were based on the following simplifying assumptions.

1. The overall reaction step is not limited by diffusion.
2. The surface of the catalyst was uniform and its activity towards the different steps (adsorption, surface reaction, and desorption) involved in the reaction was not affected by coverage.
3. There was no side (saponification) reaction.
4. The size of the catalyst pellet was small enough to ensure that the effect of diffusion on the overall reaction rate was negligible.
5. The intermediate reaction steps were very fast and did not affect the overall rate of the reaction. Hence, the intermediates (diglyceride and monoglyceride) were consumed as soon as they were formed.
6. Due to the relatively high molar concentration of methanol used with respect to triglyceride concentration, the change in the concentration of methanol was negligible.

2.5. Power Law Model

Considering a one-step transesterification, the overall reaction can be presented as shown in Equation 1.

$$\mathrm{T} + 3\mathrm{M} \rightleftharpoons \mathrm{G} + 3\mathrm{F} \qquad 1$$

T, M, G, and F represent triglyceride, methanol, glycerol, and FAME, respectively. Here the initial concentrations of the products are $C_{G0} = C_{F0} = 0$. The rate expression can be written as shown in Equation 2.

$$-\mathrm{r_T} = \mathrm{kC_TC_M^3} - k''C_GC_F^3 \qquad 2$$

where, $-\mathrm{r_T}, \mathrm{k}, \mathrm{C_T}, \mathrm{C_M}, \mathrm{C_G}$, and $\mathrm{C_F}$ = the rate of disappearance of triglyceride, reaction constant, triglyceride concentration, methanol concentration, glycerol concentration, and FAME concentration, respectively.

Based on the power law model and the assumption made, the following rate equations (Equations 3 – 6) can be deduced from Equation 2.

i. Reversible First-Order Reaction Kinetics

$$-\mathrm{r_T} = -\frac{\mathrm{dC_T}}{\mathrm{dt}} = \mathrm{k'C_T} - \mathrm{k'_2}C_GC_F^3 \qquad (3)$$

where, $\mathrm{k'} = k\mathrm{kC_M^3}$

ii. Irreversible Pseudo First-Order Reaction Kinetics

$$-\mathrm{r_T} = -\frac{\mathrm{dC_T}}{\mathrm{dt}} = \mathrm{k'C_T} \tag{4}$$

iii. Reversible Second Order Reaction Kinetics

$$-\mathrm{r_T} = -\frac{\mathrm{dC_T}}{\mathrm{dt}} = \mathrm{k'}C_T^2 - k''C_GC_F^3 \tag{5}$$

iv. Irreversible Pseudo Second Order Kinetics

$$-\mathrm{r_T} = -\frac{\mathrm{dC_T}}{\mathrm{dt}} = \mathrm{k'}C_T^2 \tag{6}$$

2.6 Regression Analysis

The rate of reaction for triglycerides was determined from experimental data at 55 °C using a graphical method. A graph of triglyceride concentration versus time was plotted, and the slope at various points on the curve, representing the rate of reaction, was calculated. The data was analyzed with POLYMATH 6.10 professional software to find the values of the model's constant terms by minimizing the sum of squared errors between observed and predicted rates [16]. Statistical indicators such as the coefficient of determination (R^2), adjusted coefficient of determination (R^2 adj), root mean square error (E_{RMS}), and variance were used to select the best-fitting model for the experimental data. These parameters were calculated using Equations (7) to (10).

$$R^2 = 1 - \frac{\sum_{i=1}^{n}(r_{obs.i} - r_{pred,i})^2}{\sum_{i=1}^{n}(r_{avobs} - r_{avpred})^2} \tag{7}$$

$$R_{adj}^2 = 1 - \left[(1 - R^2)\left(\frac{n-1}{n-k-1}\right)\right] \tag{8}$$

$$E_{RMS} = \sqrt{(\tfrac{1}{n}\textstyle\sum_{i}^{n}(r_{obs,i} - r_{pred,i})^2)} \tag{9}$$

$$Variance = \sum_{i=1}^{n}\frac{(r_{obs,i} - r_{pred,i})^2}{n-k} \tag{10}$$

where, $r_{obs,i}$ is the experimental rate of reaction for the ith run, $r_{pred,i}$ is the experimental rate of reaction for the ith run, r_{av} is the average rate of reaction, n is the number of runs conducted, and k is the number of variables to be determined.

3.0 Results and Discussion

3.1 Kinetic Modelling

The variation of glycerol concentration with time at different fixed temperatures as obtained from the UV-spectrophotometric analysis is shown in Figure 2. The concentrations of glycerol at three different temperatures increased gradually from zero to near-constant maximum concentrations over a period of 180 minutes. The rise in concentration was higher at a temperature of 65 °C. The variations in the concentration of the other reaction species with time at the corresponding temperatures were then determined from the stoichiometric relationship between them.

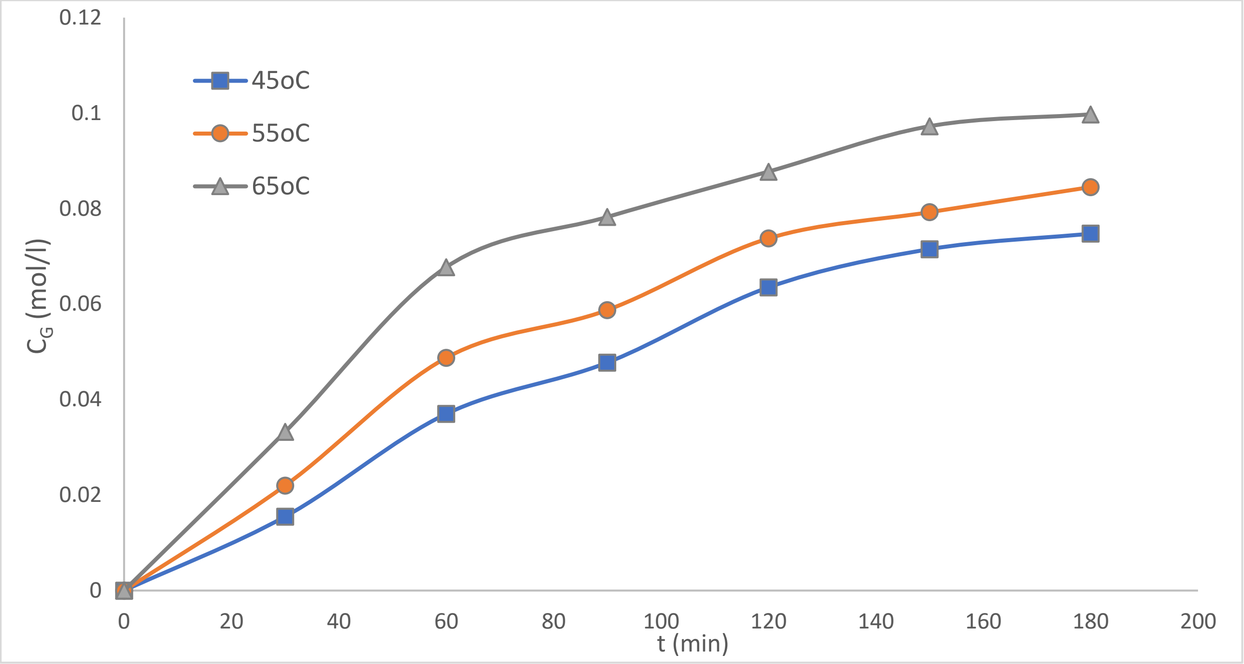

Figure 2: Concentration profile of glycerol in the transesterification of WCO

3.2 Selection of Kinetic Model

The results of the regression analysis performed on the kinetic experimental data obtained at a temperature of 55 ^oC are shown in Table 1. The selection of the best kinetic model was based on the values of their coefficient of determination (R^2 *and* R^2_{adj}) and the sum of squared errors (variance and E_{RMS}). The most suitable kinetic model is the one with the largest coefficient of determination and the smallest sum of squared error. It can be seen from Table 1 that the reversible second-order ($R^2 = 0.7742, R^2_{adj} = 0.729, E_{RMS} = 5.05E-05$, and variance $= 2.50E-08$) and pseudo-second order ($R^2 = 0.6052, R^2_{adj} = 0.6052, E_{RMS} = 6.68E-05$, and variance $= 3.64E-08$) kinetic models did not fit the experimental data and had the poorest correlations between the experimental and predicted rates. Hence, these models cannot be considered for the reaction. On the other hand, the R^2 values of the other models were well above 0.97, indicating a good fit of the experimental data. However, pseudo-first-order and Langmuir-Hinshelwood-Hougen-Watson kinetic models stood out with the highest R^2 values of 0.9829 and 0.9875, respectively. Though the R^2 value of LHHW is slightly higher than that of the pseudo-first-order kinetic model, the adjusted R^2 value of LHHW is relatively smaller. Furthermore, the variance and root mean square error of the irreversible pseudo-first-order model are also smaller than those of the LHHW model. The statistical parameters therefore suggest that the irreversible pseudo-first-order model is most suitable for the reaction kinetics. The plot of the experimental against predicted reaction rate for the irreversible pseudo-first-order model is presented in Figure 3.

Table 1: Results of the regression analysis performed on the different models

S/N	Model	Model equation	R^2	R^2_{adj}	E_{RMS}	Variance
1	Reversible first order	$-r = 0.009421C_T - 0.013848C_T C_F^3$	0.9741	0.9689	1.71E-05	2.87E-09
2	Irreversible pseudo-first-order	$-r = 0.009364C_T$	0.9829	0.9729	1.15E-05	2.50E-09
3	Reversible second order	$-r = 0.1015C_T^2 + 0.1582C_G C_F^3$	0.7742	0.729	5.05E-05	2.50E-08
4	Irreversible pseudo-second-order	$-r = 0.1043C_T^2$	0.6052	0.6052	6.68E-05	3.64E-08
5	Reversible Eley-Rideal	$-r = \frac{0.03117C_T C_M^3 - 0.3655C_G C_F^3}{(1 + 0.8949C_M + 0.3405C_G)^3}$	0.9704	0.9407	1.83E-05	5.46E-09
6	Reversible Langmuir-Hinshelwood	$-r = \frac{0.0189C_T C_M^3 - 1.1495C_G C_F^3}{(1 - 0.2356C_M - 7.5014C_G)^3(1 + 2.589C_T - 4.1957C_F)^3}$	0.9875	0.9251	1.19E-05	6.91E-09

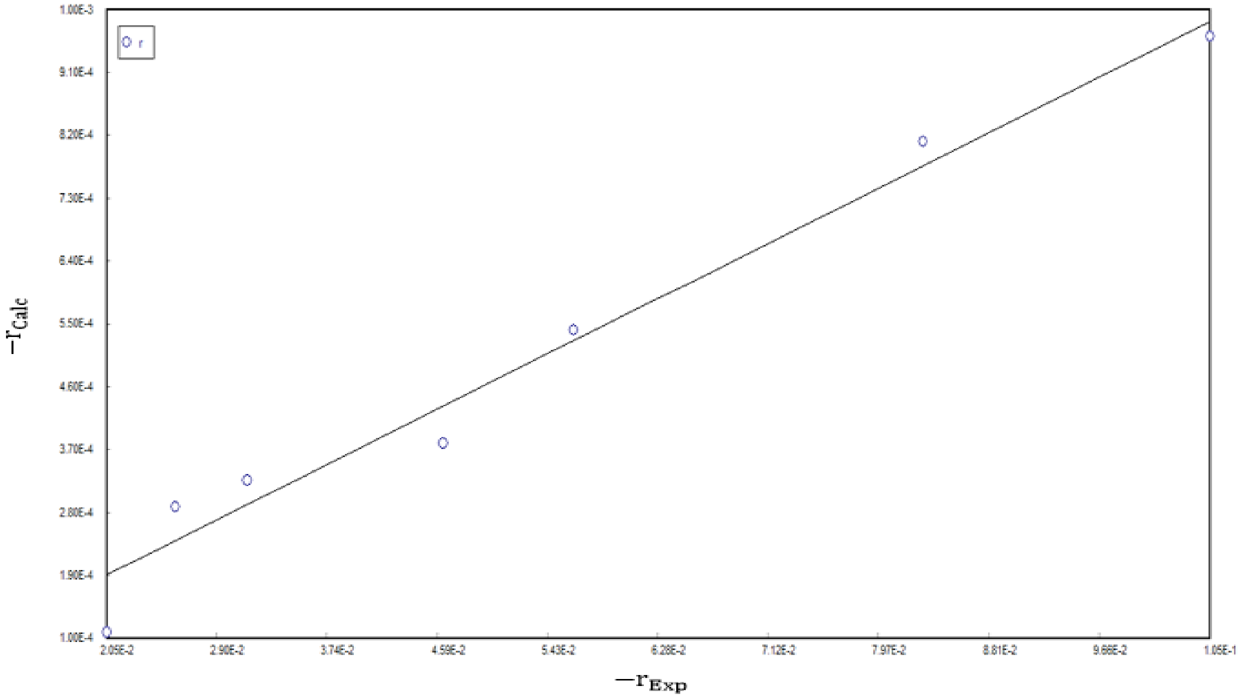

Figure 3: Experimental vs predicted reaction rate for the Irreversible pseudo-first order: $-r_T = k'C_T$

3.3 Determination of Kinetic Parameters of the Model

Having established that the kinetic model of the reaction is an irreversible pseudo-first-order whose rate equation is given by Equation (4) as:

$$-\mathrm{r_T} = -\frac{\mathrm{dC_T}}{\mathrm{dt}} = \mathrm{k'C_T}$$

Where: $C_T = C_{TO} - C_G \; so \; that \; -\frac{dC_T}{dt} = \frac{dC_G}{dt}$. With this, Equation (4) transforms to Equation (11)

$$-r_T = \frac{dC_G}{dt} = \mathrm{k'}(C_{TO} - C_G) \tag{11}$$

Upon separation of variables, Equation (11) changes to Equation (12).

$$\int_0^{C_G} \frac{1}{C_{TO} - C_G} dC_G = \mathrm{k'} \int_0^t t\, dt \tag{12}$$

Evaluation of Equation 12 gives Equation 13

$$In \left[\frac{C_{TO}}{C_{TO} - C_G}\right] = \mathrm{k'}t \tag{13}$$

The rate constant of any reaction varies with temperature. The rate constants of the transesterification of WCO over ABFC catalyst were determined at 45 ^{o}C, 55 ^{o}C, and 65 ^{o}C graphically by plotting $In\left[\frac{C_{TO}}{C_{TO}-C_G}\right]$ against t as shown in Figure 4. The slope of the straight-line graph gave the rate constant $\mathrm{k'}$at temperature T (^{o}C). The rate constants obtained were 0.0072, 0.0094, and 0.0164 min^{-1} at temperatures of 45, 55, and 65 ^{o}C respectively.

The predicted concentrations of glycerol and triglycerides as functions of time were obtained by solving the established kinetic rate equation (irreversible pseudo-first-order) with the initial conditions that C_G = 0, and C_T = 0.105 when t = 0.

$$C_G = 0.105\left(1 - e^{-\mathrm{k'}t}\right) \tag{14}$$

$$C_T = 0.105e^{-\mathrm{k'}t} \tag{15}$$

Figure 5 shows how the experimental concentration profiles of triglyceride and FAME compared with the predicted concentrations at a temperature of 65 ^{o}C ($\mathrm{k'} = 0.0164$ min^{-1}). The figure shows that the experimental and predicted concentration profiles are almost overlapping, suggesting that the chosen kinetic model can effectively and efficiently mirror the process.

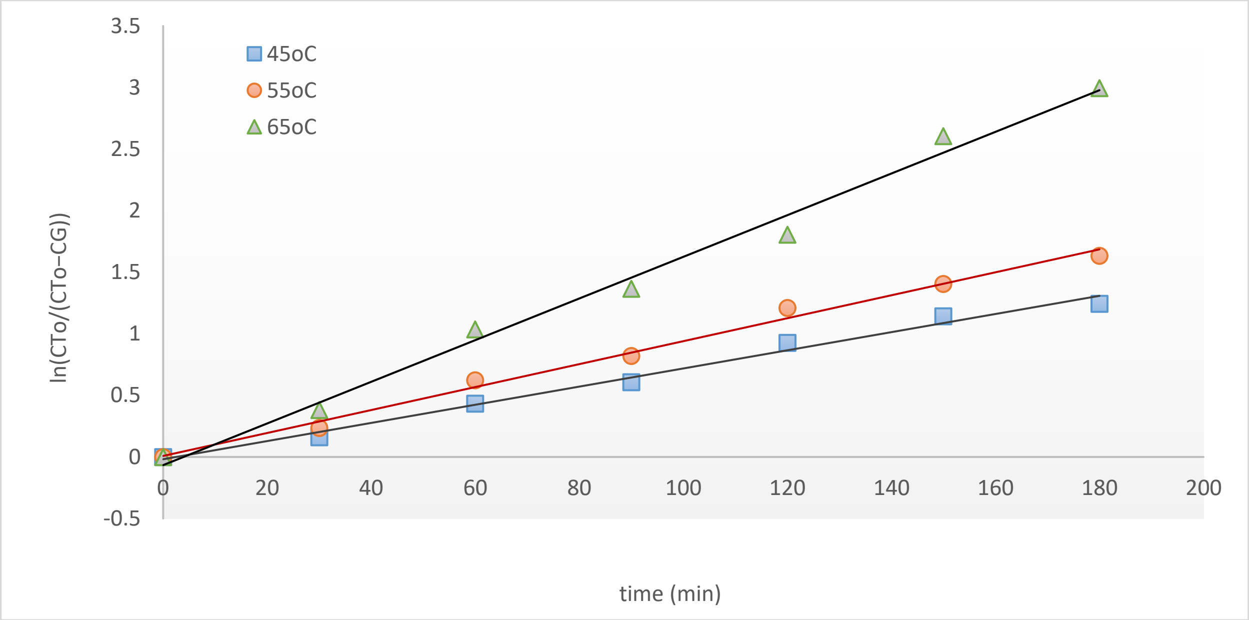

Figure 4: A plot of $In\left[\frac{C_{TO}}{C_{TO}-C_G}\right]$ against t at temperatures 45 °C, 55 °C, and 65 °C

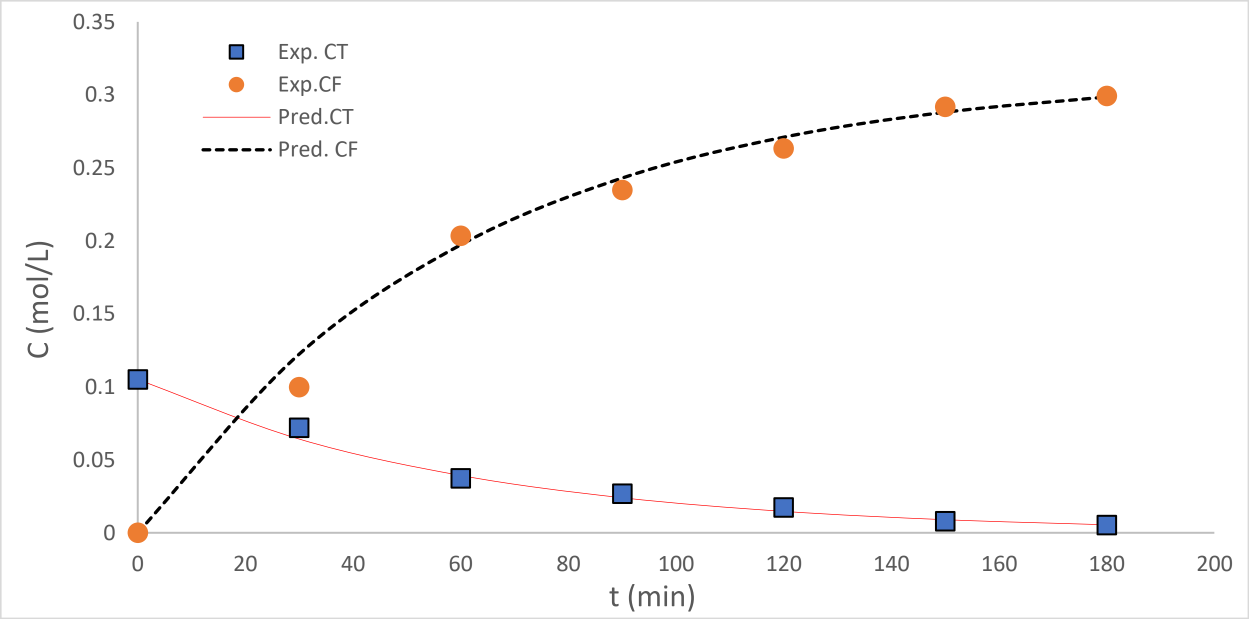

Figure 5: Experimental and predicted concentrations of triglyceride and FAME

3.4 Determination of Activation Energy of the Reaction

The activation energy of the reaction was estimated using the Arrhenius equation shown in Equation (16).

$$k' = k'_o e^{\left(-\frac{E_a}{RT}\right)} \qquad (16)$$

Where: k'_o is the pre-exponential factor or Arrhenius constant (min^{-1})

E_a is the activation energy of the reaction (KJ/mol)

R is the gas constant = 8.314×10^{-3} kJ/K.mol

T is the reaction temperature (K)

$$ln\text{k}' = lnk'_o - \frac{E_a}{R}\left(\frac{1}{T}\right) \quad (17)$$

Equation (17) was obtained from the linearization of the Arrhenius equation (Equation 16). The plot of $ln\text{k}'$ against $\frac{1}{T}$ is a straight line having a slope of $-\frac{E_a}{R}$ and intercept of lnk'_o as shown in Figure 6. The coefficient of determination value of 0.953 shows that the plot is a good fit for the experimental data. The exponential factor was calculated to be 7139.5 min^{-1} while the activation energy of the reaction was estimated as 36.6 kJ/mol. Different values of the activation energy of the transesterification reaction have been reported by different researchers. For instance, Roy *et al*. [9] reported a value of 47.13 kJ/mol for the transesterification of Ricinus communis oil over a potassium/lanthanum oxide catalyst; Zhu *et al*. [17] reported a value of 43.73 kJ/mol for the transesterification of soybean oil catalyzed by CaO/Ag, and Pugazhendhi *et al*. [18] reported activation energy of 57.82 kJ/mol for biodiesel production from WCO. The differences in the values are attributable to the fact that the value of activation energy of a reaction is a function of the nature of the feedstock and the type of catalyst employed [12]. The activation energy in the range of 33.6–84 kJ/mol has been reported in the literature as being appropriate for a heterogeneous base catalyzed transesterification [10, 11, 12, 19]. The fact that the activation energy obtained in this study is slightly lower than most of the reported values shows that the transesterification of WCO catalyzed with ABFC is not an energy-intensive process and the process is economical in terms of energy consumption. With a lower activation energy, a larger proportion of the reactant molecules have sufficient energy to overcome the energy barrier at a given temperature. This results in a faster reaction rate, enhancing the efficiency of the process. Also, lower activation energies require less energy input to initiate and sustain the reaction. This can lead to significant energy savings, reducing operational costs and making the process more environmentally friendly.

Having established the relationship between the reaction rate constant (k′) and reaction temperature, it is important that the general overall rate equation is expressed as a function of temperature to reflect the temperature-dependent nature of the reaction. Equation. (11) can now be expressed as:

$$-r_s = \frac{dC_G}{dt} = 7139.5\ \text{EXP}\left(\frac{36.6}{RT}\right)(C_{TO} - C_G) \quad (18)$$

3.5 Determination of Thermodynamics Parameters

The thermodynamic parameters of the transesterification of WCO catalyzed by ABFC were determined using the Eyring–Polanyi equation shown in Equation (19).

$$\text{k}' = \frac{k_b T}{h} e^{\left(-\frac{\Delta G}{RT}\right)} \quad (19)$$

Where: k_b is the Boltzmann constant = 1.38 × 10^{-23} J/K

T is the absolute temperature (K)

h is Planck constant = 6.626×10^{-34} J.s.

Also, $\Delta G = \Delta H - T\Delta S$

Rearrangement and linearization of Equation (19) produced Equation (20).

$$ln\frac{k'}{T} = \left(ln\frac{k_b}{h} + \frac{\Delta S}{R}\right) - \frac{\Delta H}{R}\left(\frac{1}{T}\right) \tag{20}$$

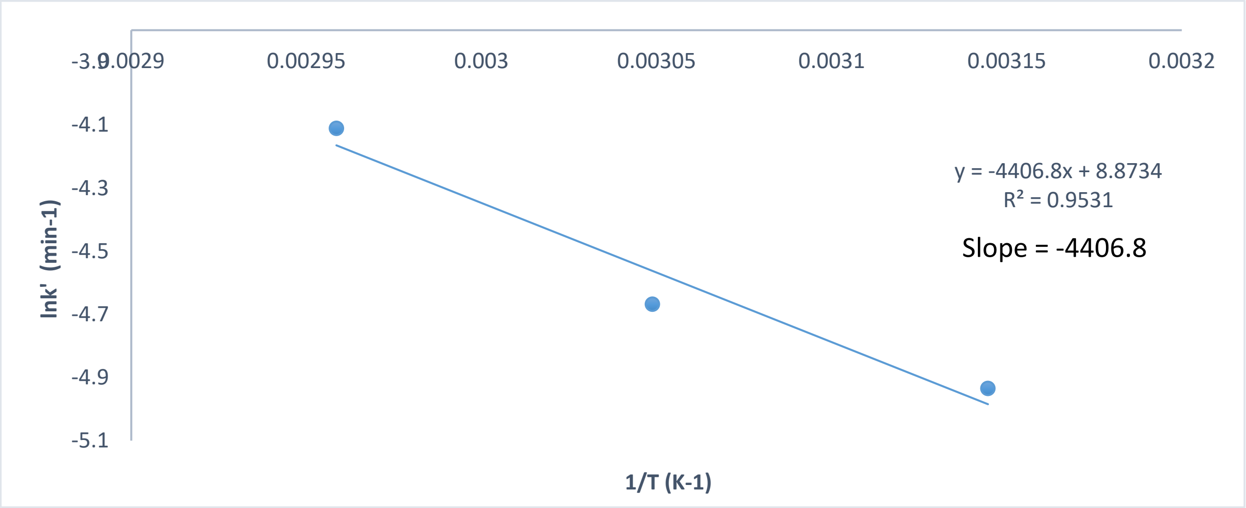

Figure 6: A plot of lnk' against $\frac{1}{T}$

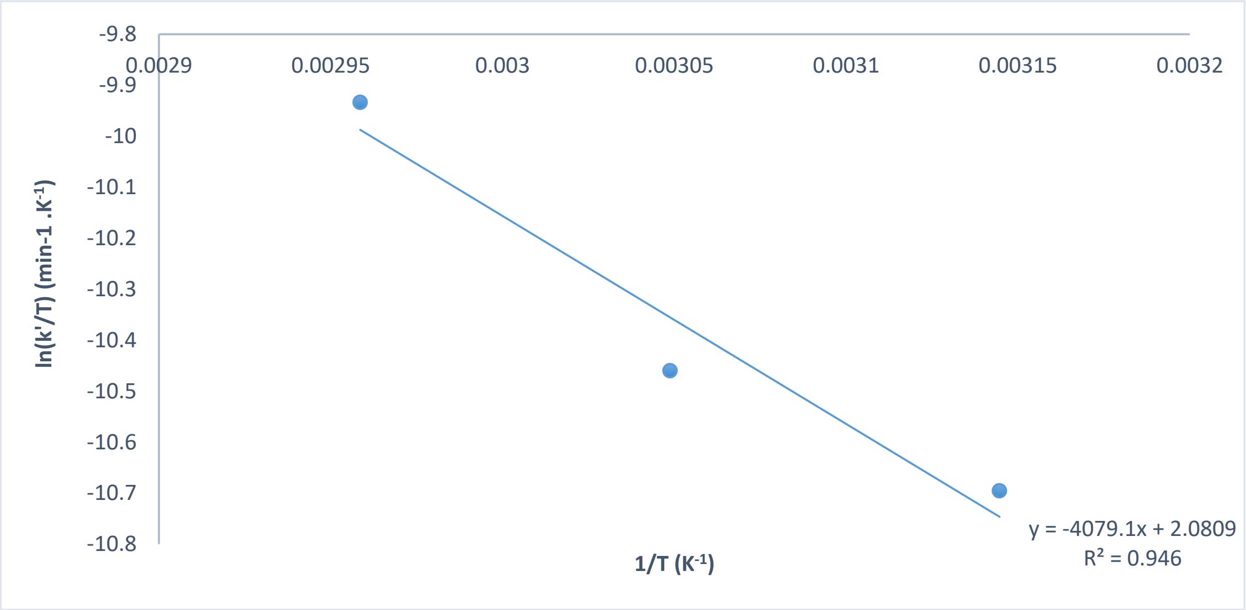

Figure 7: A lot of $ln\frac{k'}{T}$ against $\frac{1}{T}$

The plot of $ln\frac{k'}{T}$ against $\frac{1}{T}$ is a straight line with an intercept of $\left(ln\frac{k_b}{h} + \frac{\Delta S}{R}\right)$ and a slope of $-\frac{\Delta H}{R}$ as shown in Figure 7. The coefficient of correlation (R^2) of 0.946 signified that there was a good linear correlation between $ln\frac{k'}{T}$ and $\frac{1}{T}$. The change in entropy (ΔS) was calculated from the intercept while the change in enthalpy was calculated from the slope of the graph. The results of the calculation show that ΔS and ΔH of the reaction have values of -0.180 kJ/mol.K and 33.9 KJ/mol, respectively. The corresponding values of Gibb's free energy change were calculated from the expression: ΔG = ΔH - TΔS. The values of ΔG obtained were 91.1 kJ/mol, 92.94 kJ/mol, and 94.74 kJ/mol at the temperatures of 45 ^oC, 55 ^oC, and 65 ^oC, respectively. The negative nature of ΔS implied that the reactants molecules were more orderly arranged in the transition state than in the ground state [18]. The positive value of ΔH obtained signified that the transesterification of WCO catalyzed by ABFC is an endothermic reaction. Also, Gibb's free energies which were positive confirmed the non-spontaneity of the transesterification reaction. A reaction with a positive ΔG does not proceed spontaneously. External energy or work must be supplied to drive the reaction forward. Positive ΔG indicates that a reaction is not naturally favorable and requires external energy or specific conditions to proceed. Understanding this concept is crucial for manipulating and controlling chemical processes in both scientific and industrial applications. This result explains why an external heat source had to be provided for the transesterification reaction to proceed in this study.

4.0 Conclusion

This study has successfully investigated the kinetics and thermodynamics of the transesterification of waste cooking oil using a recently developed catalyst (ABFC). The transesterification reaction was found to be controlled by an irreversible pseudo-first-order kinetics whose rate equation is given as:

$$r = \frac{dC_G}{dt} = 7139.5\ \mathrm{EXP}\left(\frac{36.6}{RT}\right)(C_{TO} - C_G).$$

The reaction also proves to have a relatively low activation energy of 36.6 kJ/mol, suggesting an energy-efficient process. The thermodynamic parameters of the ABFC catalyzed transesterification of WCO are 33.9 kJ/mol and -0.180 kJ/mol. K for ΔH and ΔS respectively. The ΔG are 91.1 kJ/mol, 92.94 kJ/mol, and 94.74 kJ/mol at the temperatures of 45, 55, and 65 ^oC respectively. The reaction, therefore, is non-spontaneous, endothermic but energy-efficient process.

References

[1] Rocha-Meneses, L., Inayat, A., Latifa, A. A., Abdallah, S. A., Ghenai, C., & Kikas, T. (2023). Recent advances on biodiesel production from waste cooking oil (WCO): A review of reactors, catalysts, and optimization techniques impacting the production. Fuel, 337, 126824.

[2] Banga, M., Pathak, S., & Vinayak, V. (2023). Biodiesel production from waste cooking oil: A comprehensive review on the application of heterogenous catalysts. Renewable and Sustainable Energy Reviews, 169, 112974.

[3] Atabani, A. E., Silitonga, A. S., Badruddin, I. A., Mahlia, T. M. I., Masjuki, H. H., & Mekhilef, S. (2012). A comprehensive review on biodiesel as an alternative energy resource and its characteristics. Renewable and Sustainable Energy Reviews, 16(4), 2070-2093.

[4] Sreelekha, Dubey, N., & Avinashe, H. (2024). Utilizing Waste Cooking Oil for Sustainable Biodiesel Production: A Comprehensive Review. Journal of Scientific Research and Reports, 30(6), 222-234.

[5] Osagiede, C. A., and Aisien, F. A. (2024). Biochar-based Bi-functional Catalyst Derived from Rubber Seed Shell and Eggshell for Biodiesel Production from Waste Cooking Oil. Fuel, 358. https://doi.org/10.1016/j.fuel.2023.130076

[6] Boey, P. L., Maniam, G. P., & Hamid, S. A. (2011). Performance of calcium oxide as a heterogeneous catalyst in biodiesel production: A review. Chemical Engineering Journal, 168(1), 15-22.

[7] Tan, Y. H., Abdullah, M. O., Nolasco-Hipolito, C., & Zauzi, N. S. A. (2017). Application of RSM and Taguchi methods for optimizing the transesterification of waste cooking oil catalyzed by solid calcium oxide. Renewable Energy, 114, 437-447.

[8] Viriya-empikul, N., Krasae, P., Nualpaeng, W., Yoosuk, B., & Faungnawakij, K. (2012). Biodiesel production over Ca-based solid catalysts derived from industrial wastes. Fuel, 92(1), 239-244.

[9] Roy, T., Sahani, S., and Sharma, Y. C. (2020a). Green synthesis of biodiesel from Ricinus communis oil (castor seed oil) using potassium promoted lanthanum oxide catalyst: kinetic, thermodynamic and environmental studies. Fuel, 274, 117644. https://doi.org/10.1016/j.fuel.2020.117644

[10] Roy, T., Sahani, S., Madhu, D., and Chandra Sharma, Y. (2020b). A clean approach of biodiesel production from waste cooking oil by using single phase BaSnO3 as solid base catalyst: Mechanism, kinetics & E-study. Journal of Cleaner Production, 265, 121440. https://doi.org/10.1016/j.jclepro.2020.121440

[11] Roy, T., Sahani, S., and Sharma, Y. C. (2019). Study on kinetics-thermodynamics and environmental parameter of biodiesel production from waste cooking oil and castor oil using potassium modified ceria oxide catalyst. Journal of Cleaner Production, 119166. https://doi.org/10.1016/j.jclepro.2019.119166

[12] Putra, M. D., Irawan, C., and Ristianingsih, Y. (2018). A cleaner process for biodiesel production from waste cooking oil using waste materials as a heterogeneous catalyst and its kinetic study. Journal of Cleaner Production. https://doi.org/10.1016/j.jclepro.2018.06.010

[13] Bondioli, P., and Bella, L. D. (2005). An alternative spectrophotometric method for the determination of free glycerol in biodiesel. European Journal of Lipid Science and Technology, 107, pp. 153–157.

[14] Gong, S. (2007). Determination of Free Glycerol in Biodiesel by using PDA UV-Vis Spectrophotometer-Colorimetric method. PIN Annual Buyers' Guide, www.scinco.com

[15] Al-Sakkari, E. G., El-Sheltawy, S. T., Attia, N. K., and Mostafa, S. R. (2017). Kinetic study of soybean oil methanolysis using cement kiln dust as a heterogeneous catalyst for biodiesel production, Applied Catalysis B: Environmental, 206, pp. 146–157.

[16] Onukwuli, O. D and Ude, C. N. (2018). Kinetics of African pear seed oil (APO) methanolysis catalyzed by phosphoric acid-activated kaolin clay. Applied Petrochemical Research,https://doi.org/10.1007/s13203-018-0210-0

[17] Zhu, Z., Liu, Y., Cong, W., Zhao, X, Janaun, J., Wei, T., and Fang, Z. (2021). Soybean biodiesel production using synergistic CaO/Ag nano catalyst: Process optimization, kinetic study, and economic evaluation. Industrial Crops & Products, 166,113479

[18] Pugazhendhia, A., Alagumalai, A., Mathimani, T. and Atabani, A. E. (2020). Optimization, kinetic and thermodynamic studies on sustainable biodiesel production from waste cooking oil: An Indian perspective. Fuel, 273, 117725

[19] Feyzi, M., and Shahbazi, Z., (2017). Preparation, kinetic and thermodynamic studies of Al–Sr nanocatalysts for biodiesel production. J. Taiwan Inst. Chem. Eng., 71, pp. 145-155.

[20] Joorasty, M., Alireza Hemmati, A., and Rahbar-Kelishami, A. (2021). NaOH/clinoptilolite-Fe_3O_4 as a novel magnetic catalyst for producing biodiesel from Amygdalus scoparia oil: Optimization and kinetic study. *Fuel.* 303, https://doi.org/10.1016/j.fuel.2021.121305